EFFECTS OF HEAT SOURCE/SINK ON MAGNETOHYDRODYNAMIC FLOW AND HEAT TRANSFER OF A NON-NEWTONIAN POWER-LAW FLUID ON A STRETCHING SURFACE

by

Kishan NAIKOTI[a] and Kavitha PAGDIPELLI[b*]

[a] Department of Mathematics, Osmania University, Hyderabad, India
[b] Nalla Narashima Reddy Education Society's Group of Institutions, Ghatkesar, India

Original scientific paper
DOI: 10.2298/TSCI130616035N

Non-Newtonian boundary layer flow and heat transfer characteristics over a stretching surface with thermal radiation and slip condition at the surface is analyzed. The flow is subject to a uniform transverse magnetic field. The suitable local similarity transformations are used to transform the non-linear partial differential equations into system of ordinary differential equations. The non-linear ordinary differential equations are linearized by using quasi-linearization technique. The implicit finite difference scheme has been adopted to solve the obtained coupled ordinary differential equations. The important finding in this communication is the combined effects of magnetic field parameter, power law index, slip parameter, radiation parameter, surface temperature parameter, heat source/sink parameter, local Eckert number, temperature difference parameter, generalized local Prandtl number on velocity and temperature profiles and also the skin-friction coefficient $-f''(0)$*, and heat transfer coefficient* $-\theta'(0)$ *results are discussed. The results pertaining to the present study indicate that as the increase of magnetic field parameter, slip parameter decreases the velocity profiles, whereas the temperature profiles increases for both Newtonian and non-Newtonian fluids. The power law index and heat source/sink parameter decreases the dimensionless velocity and temperature profiles. The effect of radiation parameter, Eckert number leads to increase the dimensionless temperature. It is found that increasing the slip parameter has the effect of decreasing the skin-friction coefficient* $-f''(0)$ *and heat transfer coefficient* $-\theta'(0)$*. With the increase of power law index is to reduce the skin-friction coefficient and increase the heat transfer coefficient.*

Key words: *magnetic field parameter, power-law index, radiation parameter, stretching surface, slip-conditions, implicit finite difference scheme*

Introduction

The study of non-Newtonian fluid flow has gained considerable interest for their numerous engineering applications. Details of the behavior of non-Newtonian fluids for both steady and unsteady flow situations, along with mathematical models are studied by Astarita and Marrucci [1], and Bhome [2]. Non-Newtonian fluids have received the attention of numerous investigators due to their diverse applications. Acrivos [3] investigated the boundary-layer flows for such fluids in 1960, since then a large number of related studies have been

* Corresponding author; e-mail: pagdikavitha@gmail.com

conducted because of their importance and presence of such fluids in chemicals, polymers, molten plastics, and others. Over recent years, applications of non-Newtonian fluids in many industrial processes have been interesting. Many particulate slurries, multiphase mixers, pharmaceutical formulation, cosmetics and toiletries, paints, biological fluids, and food items are examples of non-Newtonian fluids [4 -7]. For a non-Newtonian fluid, the viscous stress is a non-linear function of the rate of deformation, and the relationship for the power-law fluids given by:

$$\tau_{xy} = \mu \left| \frac{\partial u}{\partial y} \right|^{n-1} \frac{\partial u}{\partial y}$$

where τ_{xy} is the shear stress, μ – is the consistency index, and n – the power-law index.

When $n < 1$ the fluid is described as pseudo-plastic, $n > 1$ dilatants, and when $n = 1$, it is the Newtonian fluid. Schowalter [4, 5] was the first one, who formulated the boundary layer flow of a non-Newtonian fluid and established the conditions for the existence of a similarity solution. A similarity solution to the boundary layer equations for a power-law fluid flowing along a flat plate at zero degree of angle was obtained by Acrivos *et al.* [3]. The study of flow and heat transfer generated by stretching surface in an otherwise quiescent fluid plays a significant role in many material processing applications such as hot rolling, extrusion, metal forming, wire and glass fiber drawing, and continuous casting. Boundary layer flow on a continuous moving solid surface in a Newtonian fluid has been studied by Sakiadias [8, 9]. Crane [10] has studied the boundary layer flow of a Newtonian fluid caused by the stretching surface. The momentum and heat transfer in laminar boundary layer flow of non-Newtonian fluids past a semi-infinite flat plates with the thermal dispersion in the presence of a uniform magnetic field for both the cases of static plate and continuous moving plate were analyzed by Naikoti and Borra [11]. Several researches, Gupta and Gupta [12], and Chen [13], have also studied the boundary layer flow over a stretching surface. In all of the previous studies, the influence of the thermal radiation is ignored. The radiative effects have important applications in physics and engineering. The radiation heat transfer effects on different flows are very important in space technology and high temperature process. It is important to note that all radiative properties depend strongly on wavelength. The material can be optically thick in some wavelength regions and optically thin in another. The mixed convection heat transfer in the boundary layer flow due to an exponentially stretching sheet with magnetic field and thermal radiation has been studied by Bidin and Nazar [14], and Pal [15]. If centric system involving the polymer extrusion process is placed in a thermally controlled environment, then radiation heat transfer in the system can perhaps lead to a desired product with a sought characteristic. Effects of radiation on non-Newtonian fluids has been studied by many authors, [16-21].

However, non-Newtonian fluids such as polymeric materials often exhibit slip condition on solid boundaries. For instance, when polymeric melts flow due to an applied pressure gradient, there is a sudden increase in the throughput at a critical pressure gradient. The fluid slippage phenomenon at the solid boundaries appear in many applications such as in micro-channels or nanochannels and in applications where thin films of light oil is attached to the moving plates, or when the surface is coated with special coatings such as thick monolayer of hydrophobic octadecyltrichlosilane. Navier [22] first proposed the equivalent partial slip boundary condition at the surface. Non-Newtonian flows with slip boundary condition have been studied by many investigators, [23, 24]. The study of the non-Newtonian flows with slip boundary has become active in recent, because of the wide application of such fluids in food engineering, petroleum production, power engineering, and in polymer melt and polymer solutions used in plastic processing industries. Postelnicu and Pop, [6], Sahoo and Do [25] investigated the effects of partial slip on the steady flow of an incompressible, electrically conducting third-grade fluid over to a stretching sheet taking into account magnetic field. Recently, the flow and heat transfer characteristics of a non-Newtonian power-law fluid over a stretching surface in the presence of radiation and slip condition at the surface is studied by Mostafa [26]. In this paper, the problem of flow and heat transfer characteristics of a non-Newtonian power law fluid over a stretching surface in the presence of magnetic field is investigated numerically. The effects of momentum, slip condition and thermal radiation are taken into account. The obtained similarity equations are solved numerically with the implicit finite difference scheme to show the effects of the governing parameters magnetic parameter, M, power law index, n, slip parameter, λ, radiation parameter, R, surface temperature parameter, γ, local Eckert number, Ec, temperature difference parameter, r, generalized local Prandtl number, Pr, on dimensionless velocity and temperature profiles.

Mathematical analysis

Consider a steady, laminar, incompressible, 2-D, boundary-layer flow and heat transfer of a non-Newtonian power-law fluid over a stretching non-isothermal surface in the presence of thermal radiation and slip condition at the surface. We shall consider the wall slip condition while the wall temperature jump was not considered, [27]. The fluid is considered to be a gray, absorbing emitting radiation but non-scattering medium, gravity acts in the opposite direction to the positive x-axis. The radiative heat flux from the fluid in the x-direction is considered negligible in comparison to that in the y-direction. The Rosseland approximation [16] is used to describe the radiative heat flux in the energy equation. The physical model and co-ordinate system are shown in fig. 1.

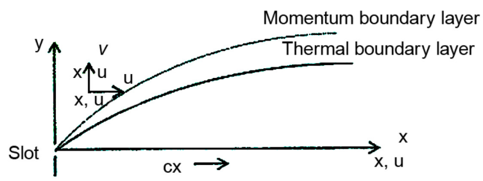

Figure 1. Physical model and co-ordinate system

The origin is located at the slot and the surface issues from the slot and moving with velocity cx in the x-direction, c being a constant having the dimension of [1/s]. The fluid occupied the upper half plane (*i. e.* $y > 0$). The governing equations within boundary layer approximations taking into account the viscous dissipation and the radiation effects in the energy equation may be written:

$$\frac{\partial u}{\partial x}+\frac{\partial v}{\partial y}=0 \tag{1}$$

$$u\frac{\partial u}{\partial x}+v\frac{\partial u}{\partial y}=\frac{\mu}{\rho}\frac{\partial}{\partial y}\left(\left|\frac{\partial u}{\partial y}\right|^{n-1}\frac{\partial u}{\partial y}\right)-\frac{\sigma B_0^2 u}{\rho} \tag{2}$$

$$u\frac{\partial T}{\partial x}+v\frac{\partial T}{\partial y}=\frac{\kappa}{\rho c_p}\frac{\partial^2 T}{\partial y^2}+\frac{\mu}{\rho c_p}\left|\frac{\partial u}{\partial y}\right|^{n+1}-\frac{1}{\rho c_p}\frac{\partial q_r}{\partial y}+\frac{Q}{\rho c_p}(T-T_\infty) \tag{3}$$

where u and v are the velocity components in the x– and y-directions, respectively, ρ – the fluid density, T – the temperature of the fluid in the boundary layer, κ – the thermal conductivity, and c_p – the specific heat at constant pressure. By using Rosseland approximation for the radiation, Raptis [17], the radiative heat flux q_r is given by:

$$q_{\mathrm{r}} = \frac{-4\sigma^*}{3k^*}\frac{\partial T^4}{\partial y} \tag{4}$$

Assuming the temperature difference within the flow is such that T^4, may be expanded in a Taylor series about T_∞ and neglecting higher order terms, we get $T^4 \cong 4T_\infty^3 T - 3T_\infty^4$, σ^* is Stefan-Boltzmann constant, and k^* – the mean absorption coefficient.

The boundary conditions for the present problem are:

$$y = 0:\ u = cx + \lambda_1\left(\left|\frac{\partial u}{\partial y}\right|^{n-1}\frac{\partial u}{\partial y}\right), \qquad v = 0, \qquad T = T_w = T_\infty + Ax^\gamma,$$

$$y \to \infty : u \to 0, \qquad T \to T_\infty \tag{5}$$

where T_w and T_∞ are the temperature of the fluid at the surface and at infinity, respectively, γ is the surface temperature parameter, A – the constant, and λ_1 – the slip coefficient having dimension of length.

By introducing the following local similarity transformations and dimensionless temperature:

$$\eta = y\left(\frac{c^{2-n}x^{1-n}}{\nu}\right)^{\frac{1}{n+1}}, \qquad \psi = \left(\nu x^{2n}c^{2n-1}\right)^{\frac{1}{n+1}} f(\eta), \qquad \theta(\eta) = \frac{T - T_\infty}{T_w - T_\infty} \tag{6}$$

where ψ is the stream function that satisfies the continuity eq. (1) and is defined by:

$$u = \frac{\partial \psi}{\partial y}, \qquad v = -\frac{\partial \psi}{\partial x} \tag{7}$$

into eqs. (1)-(3), and using eq. (4), we have:

$$nf''' \left|f''\right|^{n-1} + \frac{2n}{n+1} ff'' - f'^2 - Mf' = 0 \tag{8}$$

$$\theta'' + \Pr\left(\frac{2n}{n+1} f\theta' - \gamma f'\theta + \mathrm{Ec}\left|f''\right|^{n+1}\right) + R3r(1 + r\theta)^2\theta'^2 + (1 + r\theta)^3\theta'' + S\theta = 0 \tag{9}$$

where primes denote differentiation with respect to η, $r = (T_w - T_\infty)/T_\infty$ is temperature difference parameter (or heating factor). It is the relative difference between the surface temperature and temperature far away from the surface. At $r > 0$ for the heated surface, the fluid adjacent to the surface receives heat and becomes hot, and if $r < 0$ for the case of cooled surface, there is heat transfer from the fluid to the surface: $\nu = \mu/\rho$ is the kinematic viscosity, $R = (16\dot{\sigma}/3\dot{k}\kappa)T_\infty^3$ – the radiation parameter, $\mathrm{Ec} = cx^2/[c_p/(T_w - T_\infty)]$ the local Eckert number, $\Pr = \rho c_p/\kappa\ [(c^{3-3n}x^{2-2n})/\nu^2]^{-1/(n+1)}$ – the generalized local Prandtl number for the power law fluid, $S = Q/k\ [(c^{2-n}x^{1-n})/\nu]^{-2/(n+1)}$ – heat source/sink parameter.

It is a measure of the relative importance of heat conduction and viscosity of the fluid. The Prandtl number, like viscosity and thermal conductivity, is a material property and it thus varies from fluid to fluid.

The transformed boundary conditions are given by:

$$\eta = 0: f = 0, \quad f' = 1 + \lambda\left(\left|f''\right|^{n-1} f''\right), \quad \theta = 1, \qquad \eta \to \infty: f' \to 0, \theta = 1 \tag{10}$$

where $\lambda = \lambda_1[(c^{2n-1}x^{n-1})/v^n]^{1/(n+1)}$ is the slip parameter. More specifically, λ is the ratio between the slip coefficient λ_1 and the viscous length scale $[(c^{2n-1}x^{n-1})/v^n]^{1/(n+1)}$. If $\lambda = 0$, then generally assumed no-slip boundary condition is obtained. If λ is finite, fluid slip occurs at the surface. The parameters Pr, λ, r, and Ec correspond to local effects, *i. e.* pertaining to specific values of x. Therefore, eqs. (8) and (9) are locally similar together with the boundary conditions, eq. (10), and can be solved at given values of x, [13, 28]. To solve the system of transformed governing eqs. (8) and (9) with the boundary conditions, eq. (10), first eqs. (8) and (9) are linearized using the quasi linearization technique by Bellman and Kalaba [29]. The converted linear coupled equations are solved using implicit finite difference scheme along with Gauss-Seidel iteration method. The computations were carried out by using C programming language. Important physical parameters for this problem are the local skin-friction coefficient and local Nusselt number.

The local skin-friction coefficient is given by:

$$C_{\text{fx}} = \left(\frac{2\tau_{xy}}{\rho c^2 x^2}\right)_{y=0} = 2\ \text{Re}_x^{\frac{1}{n+1}} \left|f''(0)\right|^{n-1} f''(0) \tag{11}$$

The local Nusselt number is given by:

$$\text{Nu}_x = \frac{x\left(-\dfrac{\partial T}{\partial y}\right)_{y=0}}{T_w - T_\infty} = -\ \text{Re}_x^{\frac{1}{n+1}}\ \theta'(0) \tag{12}$$

where $\text{Re}_x = (c^{2-n}\, x^n)/v$ is the local non-Newtonian Reynolds number.

Results and discussion

The system of non-linear differential eqs. (8) and (9) are solved under boundary conditions, eq. (10), by using implicit finite difference scheme along with Gauss-Seidel iteration method. Numerical results are obtained to study the effects of the various values of magnetic parameter, M, power law index, n, slip parameter, λ, radiation parameter, R, surface temperature parameter, γ, local Eckert number, Ec, temperature difference parameter, r, and generalized local Prandtl number, Pr. The graphs for dimensionless velocity $f'(\eta)$ and temperature $\theta(\eta)$ are shown in figs. 2-12. The present results have also been compared with those of Mostafa [26] for pseudo plastic fluids ($n < 1$), Newtonian fluid for ($n = 1$) and dilatants fluids ($n > 1$). The comparison results are given in tables and found good agreement. Figures 2-12 illustrate the effect of different governing flow parameters for: (a) shear thinning fluid ($n < 1$), (b) Newtonian fluid ($n = 1$), and (c) shear thickening fluid ($n > 1$). Figure 2 indicate the velocity profile f' for Newtonian and non-Newtonian fluid. It is clear from this figure that the pronounced effect of the magnetic field parameter, M, on velocity profile, f', decreases with increase in magnetic parameter *i. e.* the Laurent force which opposes the flow leads to an enhanced declaration of the flow in both Newtonian and non-Newtonian fluids.

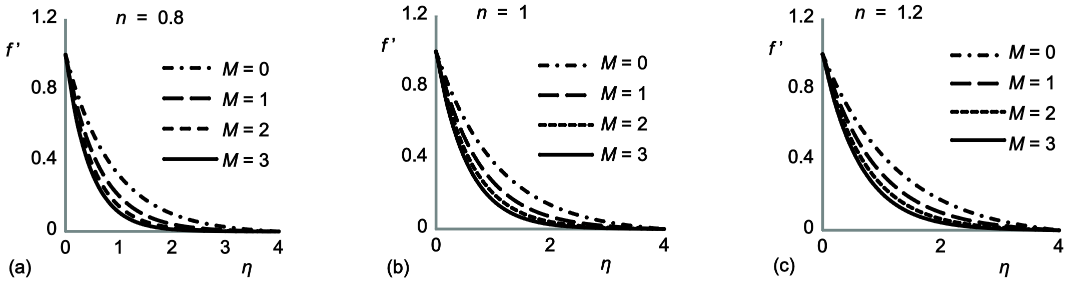

Figure 2. Velocity distribution for different values of *M*, for Pr = 10, Ec = 0.1, λ = 0.05, *R* = 0.1, *r* = 0.1, and γ = 0.05; (a) pseudoplastic fluids (*n* = 0.8), (b) Newtonian fluids (*n* = 1), and (c) dilatant fluids (*n* = 1.2)

Figure (3) displays the influence of the magnetic field parameter, M, on temperature profiles θ for: (a) pseudo plastic fluid (n = 0.8), (b) Newtonian fluid for (n = 1), and (c) dilatants fluid (n = 1.2). It can be seen that the temperature profiles increases with increase of M.

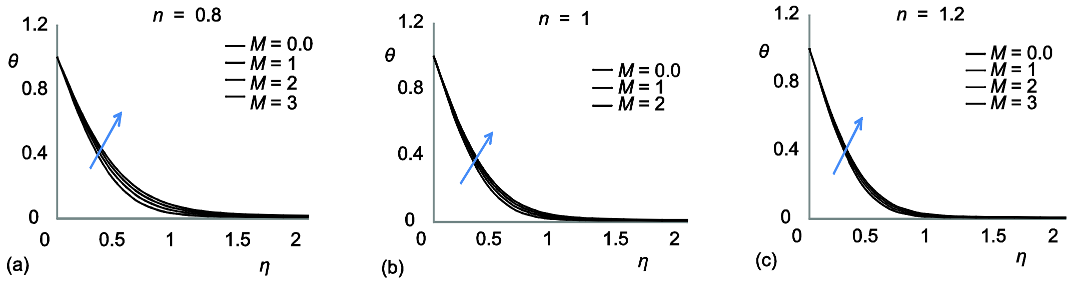

Figure 3. Temperature distribution for different values of *M*, for Pr = 10, Ec = 0.1, λ = 0.05, *R* = 0.1, and *r* = 0.1; (a) pseudoplastic fluids (*n* = 0.8), (b) Newtonian fluids (*n* = 1), and (c) dilatant fluids (*n* = 1.2)

Figure 4 elucidate the effect of the power-law index, n, on the dimensionless velocity profiles on: (a) velocity profiles and (b) temperature profiles. The results indicate that the velocity within the boundary layer decreases as n increases, a large velocity is predicted for shear thinning fluid (n < 1) and smaller velocity for shear thickening fluid (n > 1), as compared to

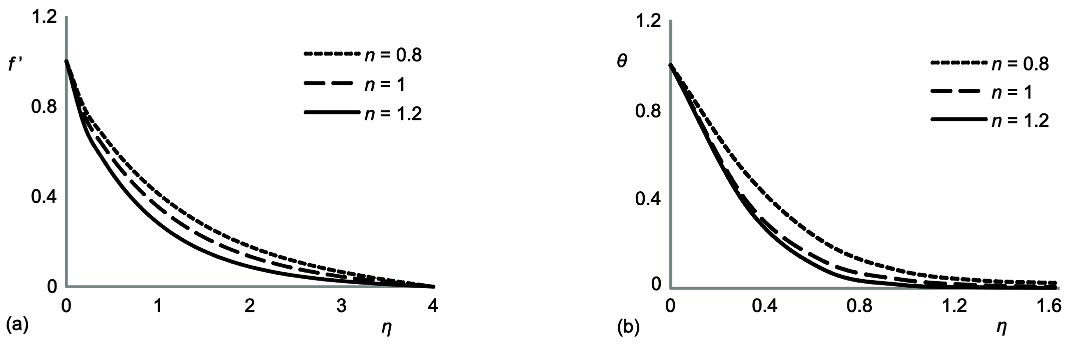

Figure 4. Velocity distribution for different values of *n*; (a) Pr = 10, Ec = 0.1, *R* = 0.1, *r* = 0.1, γ = 0.05, and *M* = 0.0; (b) Pr = 10, Ec = 0.0, *R* = 0.1, *r* = 0.1, γ = 0.5, and *M* = 0.0

Newtonian fluid (n = 1). It is also observed that the thermal boundary layer thickness decreases as n increases. It is found from fig. 4(b) that the temperature profiles decreases with increase of power-law index n. The influence of slip parameter, λ, on velocity profiles and temperature profiles are shown in figs. 5 and 6 for: (a) pseudo plastic fluid (n = 0.8), (b) Newtonian fluid for (n = 1), and (c) dilatant fluid (n = 1.2). It is interesting to find from figures that even for the presence of small amount of slip λ = 0.05, 0.1 dominates the flow condition on f' *i. e.* in presence of slip λ, f' decreases for both Newtonian and non-Newtonian fluids. Interestingly, it can be seen that in presence of slip λ the effect is less in dilatant fluids when compared with other fluids. In a subsequent fig. 6 we have seen the effect of slip parameter, λ, on temperature profiles. It is shown that increase in λ is to increase temperature profiles for both Newtonian and non-Newtonian fluids the slip parameter effect is very less in Newtonian fluid.

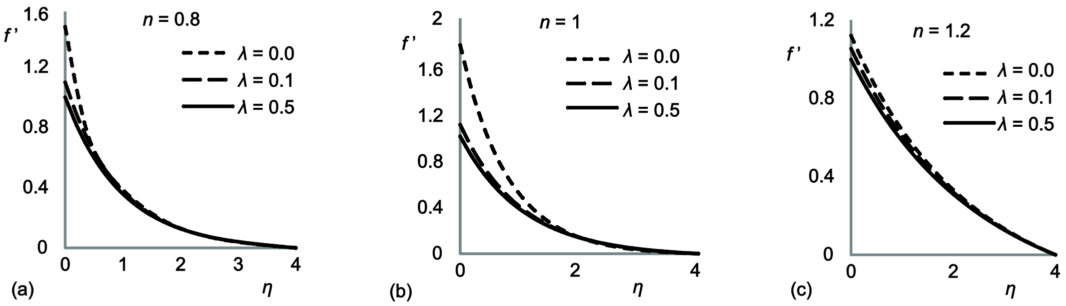

Figure 5. Velocity distribution for different values of λ, for Pr = 10, Ec = 0.0, R = 0.1, r = 0.1, γ = 0.5, and M = 0.0; (a) pseudoplastic fluids (n = 0.8), (b) Newtonian fluids (n = 1), and (c) dilatant fluids (n = 1.2)

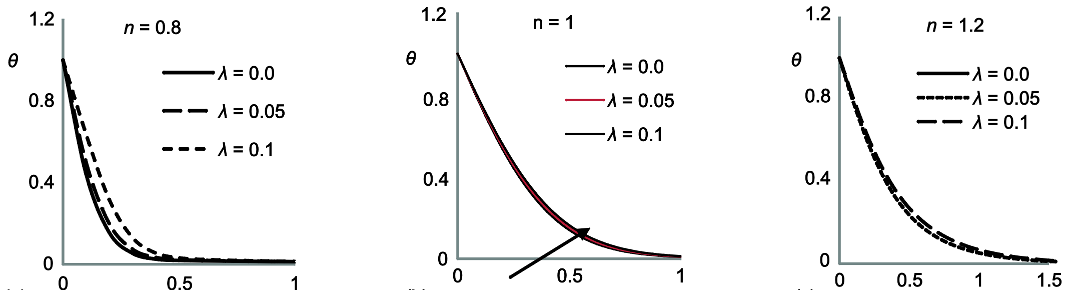

Figure 6. Temperature distribution for different values of λ, for Pr = 10, Ec = 0.0, R = 0.1, r = 0.05, γ = 0.5, and M = 0.0; (a) pseudoplastic fluids (n = 0.8), (b) Newtonian fluids (n = 1), and (c) dilatant fluids (n = 1.2)

In fig. 7 the temperature profiles θ has been plotted for different values of radiation parameter, R. It is shown from the figure that the increase in radiation parameter, R, leads to increase in temperature profiles for both Newtonian and non-Newtonian fluids. The thermal boundary layer thickness increases for pseudoplastic fluids with the influence of radiation parameter, R, is significantly increasing when compared with other fluids. Figure 8 elucidates the effects of the surface temperature γ on: (a) pseudoplastic fluid (n = 0.8), (b) Newtonian fluid for (n = 1), and (c) dilatants fluid (n = 1.2). In case of $\gamma < 0$ the dimensionless temperature increases as γ values varies from γ = 0, –5, –7, whereas for the case $\gamma > 0$ the temperature decreases with increase of γ for both Newtonian and non-Newtonian fluids is noticed.

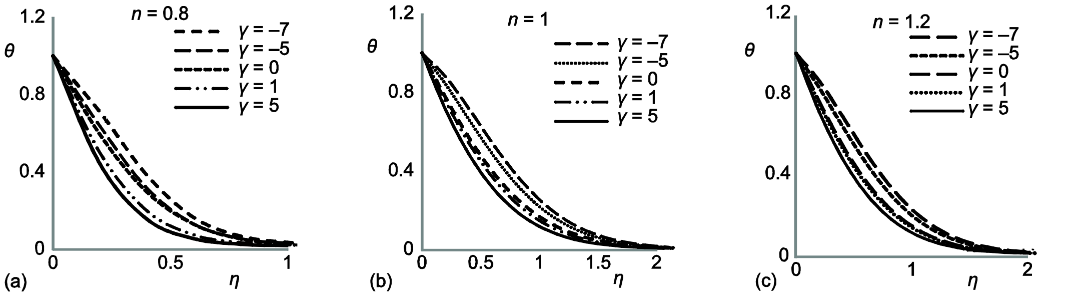

Figure 7. Temperature distribution for different values of *R*, for Pr = 10, Ec = 0.0, *λ* = 0.05, *r* = 0.1, *γ* = 0.5, and *M* = 0.0; (a) pseudoplastic fluids (*n* = 0.8), (b) Newtonian fluids (*n* = 1), and (c) dilatant fluids (*n* = 1.2)

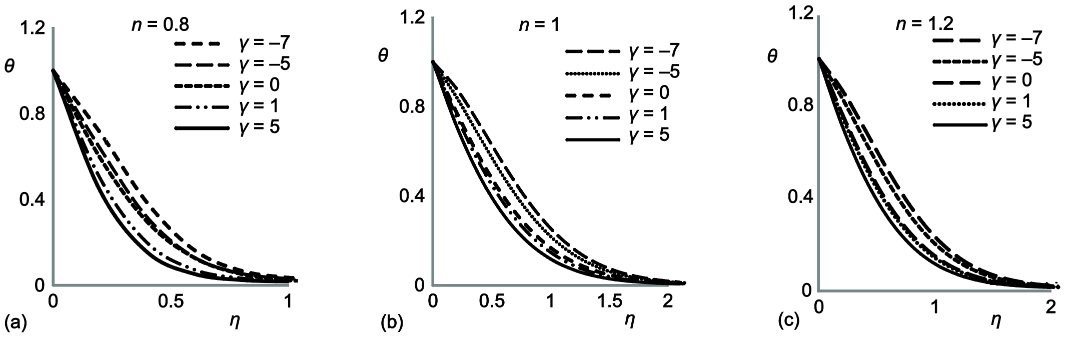

Figure 8. Temperature distribution for different values of *γ*, for Pr = 10, Ec = 0.0, *λ* = 0.05, *r* = 0.1, *R* = 0.1, and *M* = 0.0; (a) pseudoplastic fluids (*n* = 0.8), (b) Newtonian fluids (*n* = 1), and (c) dilatant fluids (*n* = 1.2)

Figure 9 indicates the effect of Eckert number on temperature profiles for: (a) pseudoplastic fluid (n = 0.8), (b) Newtonian fluid for (n = 1), and (c) dilatants fluid (n = 1.2). It is easily observed that as compared to no-viscous dissipation (Ec = 0), it can be seen that the dimensionless temperature increases as Eckert number increases. As expected one sees that the increase in fluid temperature due to viscosity is observed to be more pronounced for higher value of Eckert number. Interestingly, it is noticed that the influence of viscous dissipation is very less in Newtonian fluids when compared with non-Newtonian fluids. The effect of temperature difference parameter, r, on temperature profiles is shown in fig. 10.

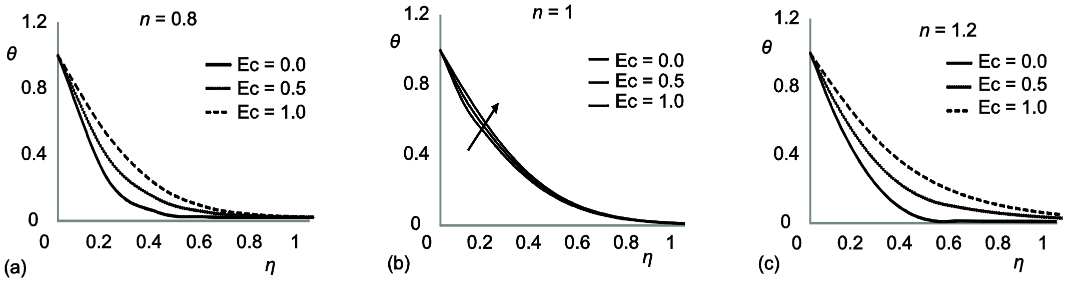

Figure 9. Temperature distribution for different values of Eckert number, for Pr = 10, *γ* = 0.05, *λ* = 0.1, *r* = 0.1, *R* = 0.1, and *M* = 0.0; (a) pseudoplastic fluids (*n* = 0.8), (b) Newtonian fluids (*n* = 1), and (c) dilatant fluids (*n* = 1.2)

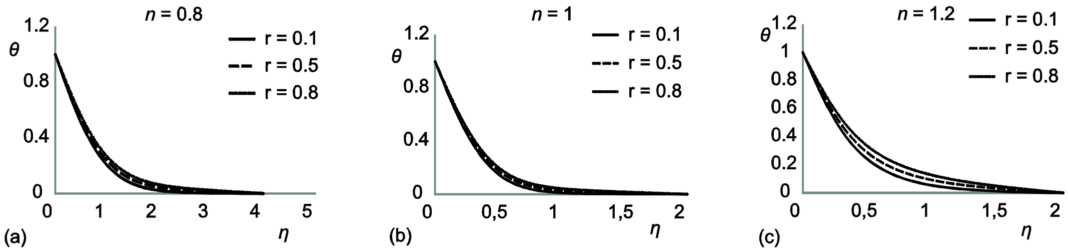

Figure 10. Temperature distribution for different values of *r*, for Pr = 10, *γ* = 0.5, *λ* = 0.05, Ec = 0.0, *R* = 0.1, and *M* = 0.0; (a) pseudoplastic fluids (*n* = 0.8), (b) Newtonian fluids (*n* = 1), and (c) dilatant fluids (*n* = 1.2)

It is noticed that the increase in difference parameter, *r,* leads to increase in temperature profiles for both Newtonian and non-Newtonian fluids. Figure 11 depicts the effects of Prandtl number on temperature profiles for Newtonian and non-Newtonian fluids. It can be seen that the temperature profiles decreases with an increase in the Newtonian Prandtl number, *i. e.*, with increase in kinematic viscosity, *ν,* on the decrease of the thermal conductivity, *κ,* for non-Newtonian fluids.

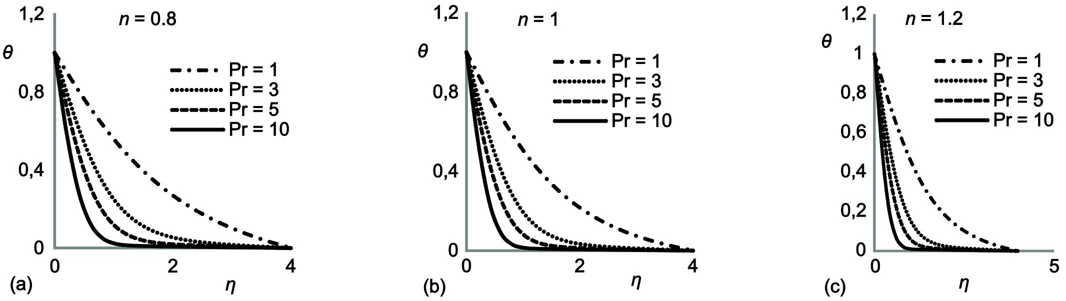

Figure 11. Temperature distribution for different values of Pr, for *γ* = 0.05, *λ* = 0.05, Ec = 0.0, *R* = 0.1, *r* = 0.1, and *M* = 0.0; (a) pseudoplastic fluids (*n* = 0.8), (b) Newtonian fluids (*n* = 1), and (c) dilatant fluids (*n* = 1.2)

Now we see the effects of heat source or sink parameter, *S,* on the temperature profiles in fig. 12. From the figure it is observed that the dimensionless temperature, *θ,* decreases for increasing strength of the heat source strength the temperature increases. So, the thickness of

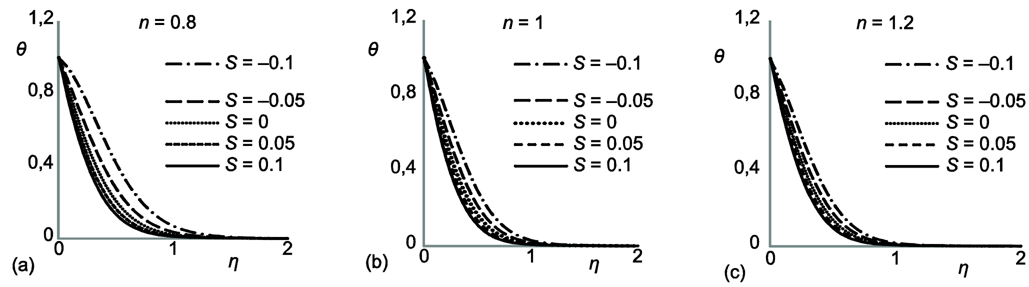

Figure 12. Velocity distribution for different values of *S*, for Pr = 10, Ec = 0.1, *λ* = 0.05, *R* = 0.1, *r* = 0.1, *γ* = 0.05, and *M* = 0; (a) pseudoplastic fluids (*n* = 0.8), (b) Newtonian fluids (*n* = 1), and (c) dilatant fluids (*n* = 1.2)

thermal boundary layer reduces for increase of heat sink parameter, but it increases with heat source parameter. This result is very much significant for the flow where heat transfer is given prime importance. The local skin-friction coefficient $-f''(0)$ decreases with increasing n or λ as can be seen from the values in tabs. 1 and 2. Also, it is seen that the local Nusselt number coefficient $-\theta'(0)$ decreases as λ increases while it increases as n increases.

Table 1. Comparison between Mostafa [26] and present values of $-f''(0)$ and $-\theta'(0)$ with Pr = 10, γ = 0.5, M = 0 for different values of λ

	$-f''(0)$		$-\theta'(0)$	
λ	Mostafa [26]	Present	Mostafa [26]	Present
0	1.0000	1.0000	3.0738	3.0737
0.1	0.8721	0.8722	2.9367	2.9366
0.2	0.7764	0.7764	0.8252	0.8251

Table 2. Values of $-f''(0)$ and $-\theta'(0)$ for different λ for M = 0, Pr = 10, R = 0.1, r = 0.1, γ = 0.5, and Ec = 0

	n = 0.8		n = 1.2	
λ	$\|f''(0)\|^n$	$-\theta'(0)$	$\|f''(0)\|^n$	$-\theta'(0)$
0	1.02402	2.7618	0.9851	2.9421
0.1	0.907	2.632	0.8517	2.8082
0.5	0.6252	2.3012	0.5705	2.4759

Conclusions

In this work the heat transfer characteristics of non-Newtonian power law fluid on a non-isothermal stretching surface with thermal radiation and MHD in the presence of wall slip is studied numerically. Using the similarity transformation the governing equations are converted to coupled non-linear system of ordinary differential equations are solved by using the implicit finite difference scheme with Gauss-Siedel iteration procedure with the help of C programming language. From the presented analysis we found that with the effect of magnetic field parameter, M, the dimensionless velocity profile, f', decreases whereas the temperature profiles increases for both Newtonian and non-Newtonian fluids. The dimensionless velocity decreases as the slip parameter, λ, increases. The temperature profiles increases with increase for both Newtonian and non-Newtonian fluids. The effect of radiation parameter, R, and temperature parameter, Eckert number leads to increase the dimensionless temperature profiles for both Newtonian and non-Newtonian fluids. The power law index, n, leads to decrease the dimensionless velocity and temperature profiles.

Acknowledgment

The authors acknowledge the financial support given through the DST-PURSE Programme of Osmania University, Hyderabad-7, A.P, India.

References

[1] Astarita, G., Marrucci, G, *Principles of Non-Newtonian Fluid Mechanic*, McGraw-Hill, New York, USA, 1974
[2] Bohme, H., *Non-Newtonian Fluid Mechanics*, North-Holland Series in Applied Mathematics and Mechanics, Elsevier Science and Technology, Amsterdam, The Netherland, 1987
[3] Acrivos, A., *et al.*, Momentum and Heat Transfer in Laminar Boundary Layer Flows of Non-Newtonian Fluids past External Surfaces, *AICHE J., 6* (1960), 2, pp. 312-317
[4] Schowalter, W. R., The Application of Boundary Layer Theory to Power-Law Pseudo Plastic Fluid Similar Solutions, *AICHE J.*, *6* (1960), 1, pp. 24-28
[5] Schowalter, W. R, *Mechanics of Non-Newtonian Fluids*, Pergamon Press, Oxford, UK, 1978
[6] Bird, R. B., *et al., Dynamics of Polymeric Liquids, Fluid Mechanics*, 2nd ed., John Wiley and Sons, New York, USA, 1987

[7] Postelnicu, A., Pop, I., Falkner-Skan Boundary Layer Flow of a Power-Law Fluid past a Stretching Wedge*, Applied Mathematics and Computation, 217* (2011), 9, pp. 4359-4368
[8] Sakiadis, B. C., Boundary-Layer Behavior on Continuous Solid Surface on a Continuous Flat Surface-I, The Boundary Layer on a Continuous Flat Surface, *AICHE J., 7* (1961a), 2, pp. 26-28
[9] Sakiadis, B. C., Boundary-Layer Behavior on Continuous Solid Surface on a Continuous Flat Surface-II, The Boundary Layer on a Continuous Flat Surface*, AICHE J.*, *7* (1961b), 2, pp. 221-225
[10] Crane, L. J., Flow Past a Stretching Plate, *ZAMP*, *21* (1970), 4, pp 645-647
[11] Naikoti, K., Borra, S. R., Quasi-Linearization Approach to MHD Effects on Boundary Layer Flow of Power-Law Fluids past a Semi Infinite Flat Plate with Thermal Dispersion, *International Journal of Non-Linear Science*, *11* (2011), 3, pp. 301-311
[12] Gupta, P. S., Gupta, A. S., Heat and Mass Transfer on a Stretching Sheet with Suction or Blowing, *Can. J. Chem. Eng., 55* (1977), 6, pp. 744-746
[13] Chen, C. H., Effect of Magnetic Field and Suction/Injection on Convection Heat Transfer on Non-Newtonian Power Law Fluids past a Power-Law Stretched Sheet with Surface Heat Flux, *Int. J. Therm. sci*., *47* (2008), 7, 954-961
[14] Bidin, B., Nazar, R., Numerical Solution of the Boundary Layer Flow over an Exponentially Stretching Sheet with Thermal Radiation, *European Journal of Scientific Research*, *33* (2009), 4, p. 710-717
[15] Pal, D., Mixed Convection Heat Transfer in the Boundary Layers on an Exponentially Stretching Surface with Magnetic Field, *Applied Mathematic and Compuation, 217* (2010), 6, 2356-2369
[16] Mansour, M. A., Gorla, R. S. R., Mixed Convection-Radiation Interaction in Power-Law Fluids along a Non-Isothermal Wedge Embedded in a Porous Medium, *Transport in Porous Media*, *30* (1998), 1, pp. 113-124
[17] Raptis, A., Flow of a Micropolar Fluid past a Continuously Moving Plate by the Presence of Radiation, *Int. J. Heat Mass Transfer*, *41* (1998), 18, pp. 2865-2866
[18] Sajid, M., Hayat, T., Influence of Thermal Radiation on the Boundary Layer Flow due to an Exponentially Stretching Sheet, *Int. J. Heat Mass Transfer*, *35* (2008), 3, pp. 347-356
[19] Siddheshwar, P. G., Mahabaleswar, U. S., Effect of Radiation and Heat Source on MHD Flow of a Viscoelastic Liquid and Heat Transfer over a Stretching Sheet, *Int. J. Non-Linear Mech*., *40* (2005), 6, pp. 807-820
[20] Abdel-Rahman, G. A., Efeects of Variable Viscosty and Thermal Conductivity on Unsteady MHD Flow of Non-Newtonian Fluid over a Stretching Porous Sheet, *Thermal Science, 17* (2013), 4, 1035-1047
[21] Sahoo, B., Poncet S., Flow and Heat Transfer of a Third Grade Fluid Past an Exponentially Stretching Sheet with Partial Slip Boundary Condition, *Int. J. Heat Mass Transfer, 54*, (2011), 23-24, p. 5010-5050
[22] Navier, C. L., *Memoire sur les lois du mouvement des fluids* (*On the Fluid Movement Laws* – in French), *Mem. Acad. R. Sci. Inst. Fr.*, (1827), 6, pp. 389-440
[23] Ariel, P. D., *et al*., The Flow of an Elastic-Viscous Fluid Past a Stretching Sheet with Partial Slip, *Acta Mechanica*, *187* (2006), 1-4, pp. 29-35
[24] Hayat, T., *et al*., The Effect of the Slip Condition on Flows of an Oldroyd 6-Constant Fluid, *Journal of Computational and Applied Mathematics*, *202* (2007), 2, pp. 402-413
[25] Sahoo, B., Do, Y., Effects of Slip on Sheet-Driven Flow and Heat Transfer of a Third Grade Fluid Past a Stretching Sheet*, Int. Communications in Heat and Mass Transfer*, *37* (2010), 8, pp. 1064-1071
[26] Mostafa, A. E.-H. M., Slip Effects on Flow and Heat Transfer of a Non-Newtonian Fluid on a Stretching Surface with Thermal radiation, *International Journal of Chemical Reactor Engineering*, *6* (2008), 1, pp. 1-20
[27] Ngoma, G. D., Erchiqui, F., Heat Flux and Slip Effect on Liquid Flow in a Microchannel*, Int. J. Therm. Sci*., *46* (2007), 11, 1076-1083
[28] Chamkha, A. J., Thermal Radiation and Buoyancy Effects on Hydromagnetics Flow over an Acceleration Permeable Surface with Heat Source or Sink, *Int. J. of Eng. Sci., 38* (2000), 5, 1699-1712
[29] Bellman, R. E., Kalaba, R. E., *Quasi-Linearization and Non-Linear Boundary Value Problem*, Elsevier, New York, USA, 1965

Paper submitted: June 16, 2013
Paper revised: February 1, 2014
Paper accepted: March 3, 2014